Hindawi
Geofluids
Volume 2022, Article ID 3917846, 17 pages
https://doi.org/10.1155/2022/3917846

Research Article

Risk Prediction of Coal and Gas Outburst Based on Abnormal Gas Concentration in Blasting Driving Face

Liming Qiu,[1,2,3,4,5] **Yujie Peng**,[1,2] **and Dazhao Song**[1,2,3]

[1]*State Key Laboratory of the Ministry of Education of China for High-Efficient Mining and Safety of Metal Mines, University of Science and Technology Beijing, Beijing 100083, China*
[2]*School of Civil and Resources Engineering, University of Science and Technology Beijing, Beijing 100083, China*
[3]*Research Institute of Macro-safety Science, University of Science and Technology Beijing, Beijing 100083, China*
[4]*State Key Laboratory Cultivation Base for Gas Geology and Gas Control (Henan Polytechnic University), Jiaozuo 454000, China*
[5]*Shaanxi Key Laboratory of Prevention and Control Technology for Coal Mine Water Hazard, Xi'an 710077, China*

Correspondence should be addressed to Yujie Peng; peng_yujie0624@126.com

Received 23 December 2021; Accepted 30 March 2022; Published 22 April 2022

Academic Editor: Xuelong Li

In order to realize dynamic, continuous, and real-time prediction of coal and gas outburst risk in real time in blasting driving face, an outburst risk prediction method based on the characteristics of gas emission after blasting is proposed. In this study, the causes of abnormal gas concentration in blasting driving face are analyzed, and the identification method of abnormal gas concentration based on weighted K-nearest neighbor (weighted KNN) is proposed. The correlation between gas emission characteristics after blasting and K_1 value is analyzed, and the prediction model of outburst risk based on convolutional neural networks (CNN) is established and applied in Jinjia coal mine in China. The results show that the causes of abnormal gas concentration mainly include ventilation stop, blasting operation, sensor adjustment, and other abnormalities. The accuracy of the identification method is 86.1%. Especially, the identification accuracy of blasting operation is 92%. There are strong correlations between the growth rate, peak value, and decay rate of gas concentration after blasting and K_1 value, and the maximum correlation coefficient is 0.92. Using the prediction model, 28 times of jet holes and 1 small outburst event are predicted successfully, and the efficiency of the prediction model is 76.39%. By this technology, the utilization rate of gas information is improved, and the relationship between the change characteristics of gas concentration after blasting and the risk of coal seam outburst is established, which is of significant for improving the prediction accuracy and risk management ability of coal and gas outburst.

1. Introduction

Coal and gas outburst is one of the most destructive and harmful dynamic disasters in coal mining. During the mining process, a large amount of coal and gas bursts out from coal seam in a very short time, accompanied by a strong dynamic phenomenon, which can cause significant personal casualties and property losses [1, 2]. With the increasing complexity of mining geological and technical conditions, coal and rock dynamic disasters such as coal and gas outburst also increase [3, 4]. Coal and gas outburst accidents caused by coal roadway driving pose a great threat to the personal safety of miners and the safety production of coal mine [5]. The technical processes adopted to prevent coal and gas outburst in the driving process are complex and various, which seriously affects the driving speed, and easily lead to the imbalance of mining proportion and the difficulty of mining replacement [6, 7].

In the major coal-producing countries, a lot of material and financial resources have been invested to conduct extensive and in-depth research on the prevention and control of coal and gas outburst ([8–10]). Many achievements have been made worldwide in the monitoring, early warning, and prevention of coal and gas outburst, and the corresponding prediction methods and early warning indicators have been put forward ([11, 12]

In the 1960s, the former Soviet Union took the lead in putting forward the single index method and comprehensive

index method for regional prediction of coal and gas outburst risk in the world through the study of coal seams with coal and gas outburst risk [13], which are mainly completed through the drilling cuttings index. The Donetsk Institute of Technology Ukraine also used the elastic modulus and shear modulus of coal to determine the coal and gas outburst risk of coal seams. Poland mainly used the two indexes of drilling cuttings and borehole gas analysis to determine the risk of coal seam outburst. It was considered that when the amount of coal powder drilling cuttings was greater than 4 g/L and the borehole gas analysis was greater than 1.18 kPa, the coal seam has the risk of coal and gas outburst. In Germany, this index is the desorbable gas content of coal seams, which is mainly measured by geological borehole sampling, and the index is used to predict the regional risk of coal and gas outburst.

In China, the traditional prediction indexes include gas analysis index Δh_2, drilling cuttings S, initial gas emission velocity q, and comprehensive index R. The popularization and application of these prediction indicators have produced good economic and social benefits in a certain period of time [14], but the amount of information obtained by these static indicators is limited, which is difficult to reflect the whole process of prominent evolution [15]. It is urgent to find a dynamic and continuous outburst risk prediction method for the risk management and prevention of coal and gas outburst.

In recent years, more and more scholars have studied the characteristics of coal and gas outburst, trying to find a method for accurately predicting outburst risk. Some experts and scholars apply engineering technologies and geophysical methods to predict the outburst risk, including the drill cuttings index method (the amount of drill cuttings S, the drill cuttings desorption index K_1 or Δh_2), the initial velocity of gas emission from drilling holes, the composite index method [16, 17], acoustic emission (AE) technology [12, 18, 19], microseismic (MS) technology [20, 21], and electromagnetic radiation (EMR) technology [22, 23]. Some scholars input factors affecting coal and gas outburst into algorithms and models of machine learning such as Fisher Discriminant Analysis (FDA) [24] and neural network [25] to analyze the correlation between various factors and the risk of coal and gas outburst and realize the prediction of outburst risk [26, 27]. Some scholars propose several new parameters, such as temperature [28], radon concentration [29], and oxygen concentration [30], as the prediction indicators of coal and gas outburst risk.

The above technologies and methods are of great significance to predicting outburst risk. However, the above research is mainly conducted for fully mechanized mining faces. For some blasting mining faces, the risk of the coal seam is also affected by blasting behavior. On the one hand, after blasting, the coal structure becomes loose, and the gas in front of the driving face gushes out, resulting in a rapid increase of roadway gas concentration, and the gas concentration would exceed the limit. On the other hand, if the speed of gas gushing out is too fast, it might drive the coal to come out together, causing coal and gas outburst disasters. At present, the general understanding of the evolution process of coal and gas outburst is that the gas bearing coal body deforms and destroys under the action of stress and gas pressure, which causes the gas to drive the coal body to gush out, resulting in disasters and accidents. Therefore, the abnormal gas concentration can predict the risk of coal seam outburst.

At present, almost all mines are equipped with safety monitoring systems, which can continuously obtain the real-time parameters of gas, wind speed, etc. It is found that when the wind speed at the local fan outlet is relatively constant and the gas sensor is hung correctly, the gas concentration measured by the gas sensor can reflect the gas desorption capacity, the disturbance desorption capacity after blasting, coal seam gas pressure coupled with mining stress, and other outburst influencing factors. On the one hand, the abnormal increase of gas concentration after blasting shows that the area has a high outburst risk [31]. On the other hand, blasting can loosen coal and cause gas release; the rapid increase of gas concentration after blasting is not necessarily caused by the strong risk of gas outburst of coal seam. Therefore, the key to effectively predict outburst is to accurately judge the abnormal gas emission caused by strong outburst risk. In the past, workers mainly focused on the concentration value of gas data and considered that high concentration is dangerous and low concentration is safe, resulting that the gas data characteristics not being fully excavated. So far, there have been few reports on the direct relationship between the change characteristics of gas concentration after blasting and the risk of coal seam outburst. In order to realize the automatic and intelligent identification of coal and gas outburst risk in blasting face, it is necessary to identify blasting events through gas concentration monitoring data, analyze the correlation between abnormal gas concentration and coal and gas outburst risk through a large amount of data, and then make accurate early warning in time.

Based on a large number of gas concentration monitoring data in safety monitoring systems of Jinjia coal mine, this paper firstly analyzes the causes of abnormal gas concentration in blasting driving face and proposes the identification method of abnormal gas concentration. Then, the correlation between gas emission characteristics after blasting and the index K_1 value reflecting outburst is analyzed, and the prediction model of coal and gas outburst risk is established. Finally, the prediction model is applied, and its prediction results are evaluated. As a supplement to the existing prediction methods, it is of great significance to improve the prediction and risk management ability of coal and gas outburst accidents.

2. Principle and Process of Gas Abnormal Identification for Outburst Risk Prediction

2.1. Identification of Abnormal Gas Concentration

2.1.1. Analysis of Abnormal Gas Concentration. The gas concentration curve reflects the change of gas concentration with time. Any fluctuation of the gas concentration curve reflects some change in downhole environment. In a large

number of historical data of gas concentration, most of monitoring data are relatively stable, and the information contained is relatively scarce. What attracts people's attention is often the abnormal data with violent fluctuations. In order to detect the time series of abnormal gas concentration, the causes of abnormal gas concentration are analyzed.

Gas monitoring system is a system used to monitor gas concentration and change to prevent gas accidents. Combined with field observation and the data in gas monitoring system, the characteristics of gas data corresponding to different types of activities are obtained.

For the blasting driving face, there are four main causes for abnormal gas time series: gas sensor adjustment, blasting operation, ventilation stop, and other abnormalities, which are shown in Figure 1 together with the stationary data.

Stationary data is a frequent pattern in the gas time series. This series is the gas time series in the period of no abnormal activity. The observed value of gas concentration is usually low and has slight fluctuation. When the gas sensor is being adjusted, the gas concentration curve rises instantaneously and lasts for a short time. When blasting mining, a large amount of gas will be released from the coal body that suddenly collapses, and the gas concentration will increase and then decrease slowly. When the working face is in the air stop state, the gas concentration will rise sharply and last for a while because the gas cannot be discharged. In addition, when the gas concentration is in an abnormal state, the concentration value varies from large to small.

It should be noted that stationary data does not mean that it is a safe signal. Whether the value of stationary data exceeds the alarm value or always shows an upward trend, it means that the risk is increasing.

In the above four cases, the gas concentration will be abnormal, but the reasons are different, and specific measures need to be taken according to the specific reasons, which cannot be treated indiscriminately. If it is determined that the gas sensor is adjusted or the gas concentration is increased due to blasting, it does not need to be treated. If the gas concentration increases due to ventilation failure, ventilation needs to be restored as soon as possible. However, if the result of outburst prevention inspection shows that the gas is abnormal and there is a risk of outburst, it is necessary to immediately strengthen ventilation and drainage, cut off power, and evacuate people. Therefore, the correct classification and identification of the abnormal state of gas concentration in the blasting driving working face are of great significance to coal mine safety production.

2.1.2. Identification Method. In the actual production process of coal mine, more attention is paid to the abnormal state with high gas concentration value. There are different ventilation and geological conditions in the different mine, and the values of gas concentration time series in the same state may also be different. Therefore, it is necessary to determine the threshold C_L according to different mine and roadway conditions to divide the gas concentration time series into gas concentration abnormal signal, that is, the gas concentration value higher than C_L in the whole gas concentration time series is defined as gas concentration abnormal signal. Set the gas concentration time series as

$$C(t) = \{C_1(t_1), C_2(t_2), C_3(t_3), \cdots, C_n(t_n)\}, \quad (1)$$

where t_i is time, $C_i(t_i)$ is the gas concentration at t_i (%) and N is the time length of gas concentration time series.

The j^{th} subsequence of $C(t)$ is

$$C_j(t) = \left\{C_{m+1}(t_{m+1}), C_{m+2}(t_{m+2}), \cdots, C_{m+p}\left(t_{m+p}\right)\right\}. \quad (2)$$

If the gas concentration value in $C_j(t)$ is continuous and $C_i \geq C_L$, the $C_i(t_i)$ in $C_j(t)$ is defined as gas concentration abnormal signal.

Gas concentration monitoring is a continuous process. The generation of gas concentration abnormal signal is closely related to the change of gas concentration in the early stage. Therefore, when extracting the characteristics of gas concentration abnormal signal, the changes of gas concentration before and after gas concentration abnormal signal should be considered to reflect its characteristics more comprehensively.

Identify the wave peak of the gas concentration abnormal signal, and intercept the gas concentration data $C_q(t)$ of $(M+N)$ min, which includes the gas concentration abnormal signal $C_j(t)$, M min before the peak, and N min after the peak. $C_q(t)$ is defined as gas concentration abnormal sequence:

$$C_q(t) = \{C_M, C_N\}, \quad (3)$$

where C_M and C_N are gas concentration time series with time length of M min and N min, respectively. The interception process of abnormal gas concentration sequence is shown in Figure 2.

The identification of abnormal gas concentration in blasting driving faces can be regarded as a classification problem. When the gas concentration value exceeds a certain threshold, determine the abnormal causes according to the change of gas concentration curve at this time. Feature extraction is a key step in the design of a classifier. The quality of features directly affects the classification performance of the classifier. It can be seen from Figure 1 that the gas concentration time series curves vary greatly under different causes. Extract the gas concentration value in $C_q(t)$, and calculate the time-domain features representing the curve change, as shown in Table 1.

Label the extracted 12 features that reflect curve changes. That is, it can accurately determine which type of sensor adjustment, blasting operation, ventilation stop, and other abnormalities belongs to each group of features. In this paper, the time corresponding to abnormal gas concentration signal peak is used to compare the sensor adjustment recording time, blasting registration recording time, and ventilation stop time (the time when the wind speed is 0). Considering the influence of error, if the time difference of comparison is less than 10 min, the labels corresponding to this group of features are sensor adjustment, blasting

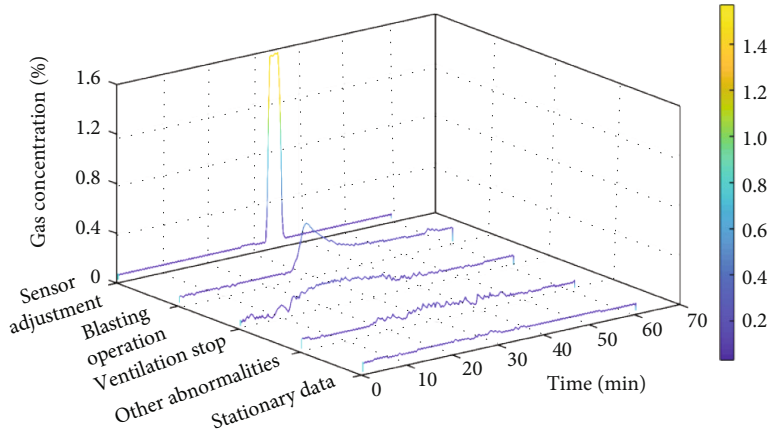

Figure 1: Time series of gas concentration for different causes.

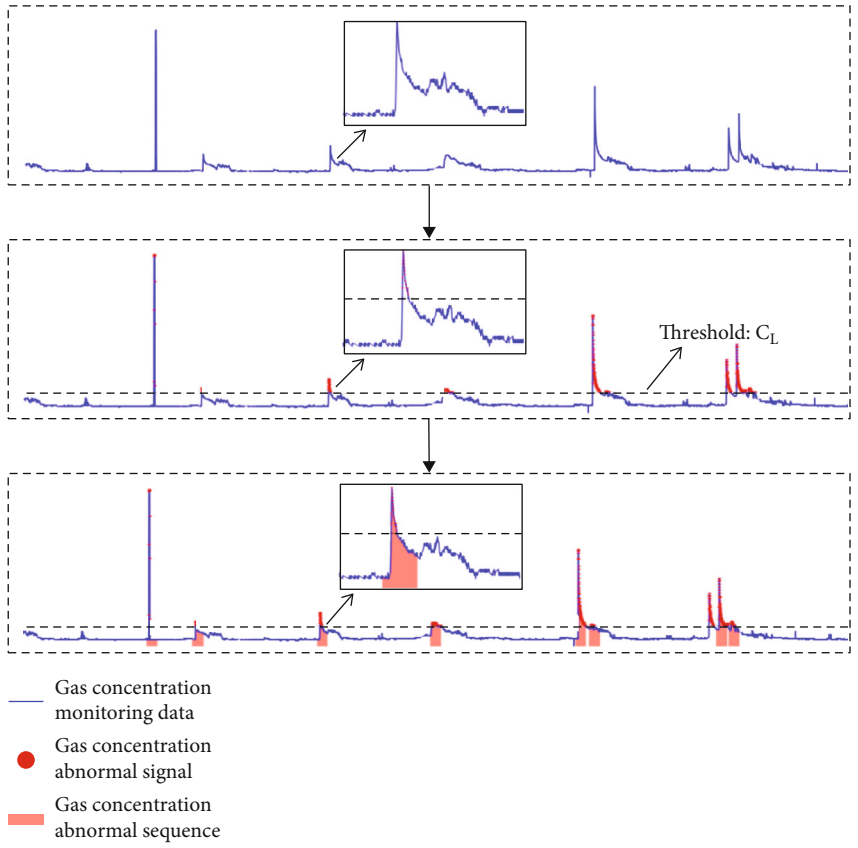

Figure 2: The interception of abnormal gas concentration sequence.

operation, and ventilation stop, respectively; others are classified as other abnormalities.

As shown in Figure 3, in total, 12 features are extracted from the abnormal gas concentration sequence and input into the weighted K-nearest neighbor (weighted KNN) classifier to realize the identification of abnormal gas concentration.

2.2. Prediction Process of Coal and Gas Outburst Risk. Based on a large number of gas concentration data in the monitoring system, an identification method of abnormal gas concentration based on weighted KNN is proposed. Based on the blasting operation in the identification results, the convolutional neural networks (CNN) is applied to establish the prediction model of coal and gas outburst risk to realize dynamic and continuous prediction of the outburst risk in front of the blasting working face. The specific process is shown in Figure 4.

The gas concentration data uploaded by the gas sensor is analyzed and judged by the method in Section Section 2.1.2.

Table 1: Time-domain features of abnormal gas concentration sequence.

Number	Features	Meaning	Calculation formula
1	Peak value	Maximum gas concentration value in $C_q(t)$	$C_{peak} = \max(C_i(t_i)), i = 1, 2, \cdots, m+n$
2	Average value	General level and central trend of gas concentration value in $C_q(t)$	$\bar{C} = 1/m+n\sum_{i=1}^{m+n} C_i(t_i), i = 1, 2, \cdots, m+n$
3	Root mean square value	Dispersion degree of gas concentration value in $C_q(t)$	$C_{rms} = \sqrt{1/m+n\sum_{i=1}^{m+n} C_i(t_i)^2}, i = 1, 2, \cdots, m+n$
4	Variance	Deviation between $C_q(t)$ and its average value	$\sigma^2 = 1/m+n\sum_{i=1}^{m+n}(C_i(t_i)-\bar{C})^2, i = 1, 2, \cdots, m+n$
5	Standard deviation	Dispersion degree of gas concentration value in $C_q(t)$	$s = \sqrt{\sigma^2}$
6	Coefficient of variation	Relative statistics of the dispersion degree of $C_q(t)$	$V_s = s/\bar{C}$
7	Peak-to-average ratio	Extreme degree of C_p in $C_q(t)$	$C_p = C_{peak}/C_{rms}$
8	Skewness	Skew direction and degree of $C_q(t)$ distribution, digital feature of the asymmetric degree of data distribution	$S_k = 1/m+n\sum_{i=1}^{m+n}\left(\left[C_i(t_i)-\bar{C}\right]^3/\sigma^3\right), i = 1, 2, \cdots, m+n$
9	Kurtosis	The sharpness of the peak of the gas concentration curve	$K = 1/n\sum_{i=1}^{m+n}\left(\left[C_i(t_i)-\bar{C}\right]^4/\sigma^4\right), i = 1, 2, \cdots, m+n$
10	Integral of a discrete sequence	The amount of gas emission during the period When the wind speed is constant	$Q = \sum_{i=t}^{T} C_i(t_i)(t_{i+1}-t_i), i = 1, 2, \cdots, m+n-1$
11	Peak width	Width of the wave crest in $C_q(t)$	C_w
12	Peak prominence	Prominence of the wave crest in $C_q(t)$	C_p

Note, m and n are, respectively, the number of gas concentration values within M and N min; Δt is the sampling interval time; t is the sampling start time; and T is the total sampling time.

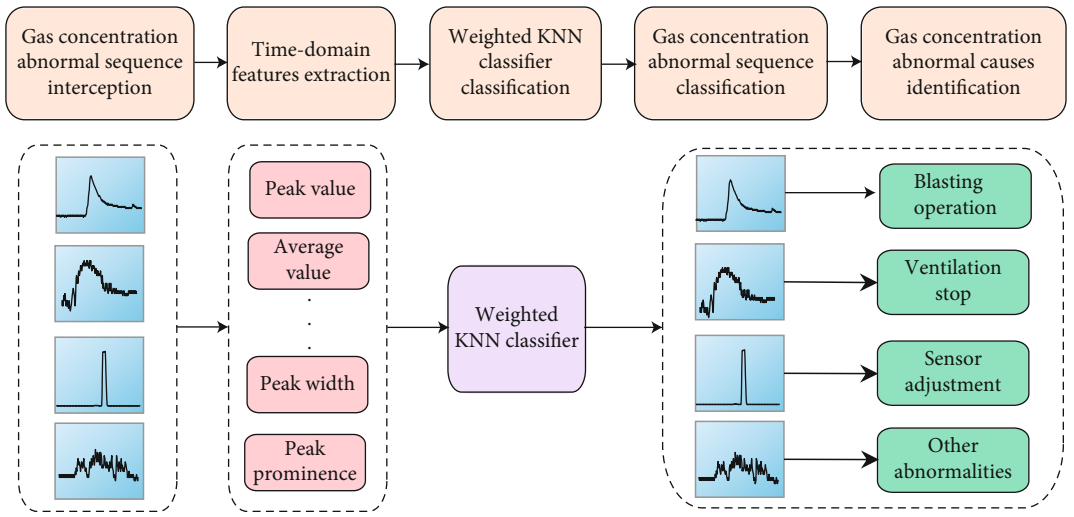

Figure 3: Identification method of abnormal gas concentration.

If the data is stationary data, no warning will be given. If not, it will be regarded as the abnormal sequence. The abnormal features will be extracted from the abnormal sequence, and then the abnormal gas concentration will be identified by the method of abnormal gas concentration based on weighted KNN. And then the gas concentration data will be converted into 2D image conversion. The 2D image conversion is used to predict the risk of coal and gas outburst in the process of coal roadway driving based on the CNN model, and the prediction results are obtained.

In order to realize dynamic and continuous prediction of coal and gas outburst risk, the weighted KNN and CNN algorithms are used to realize the abnormal gas concentration identification and outburst risk prediction. Weighted KNN [32] is an improved algorithm based on the K-nearest neighbor and uses the weight approach to assign a

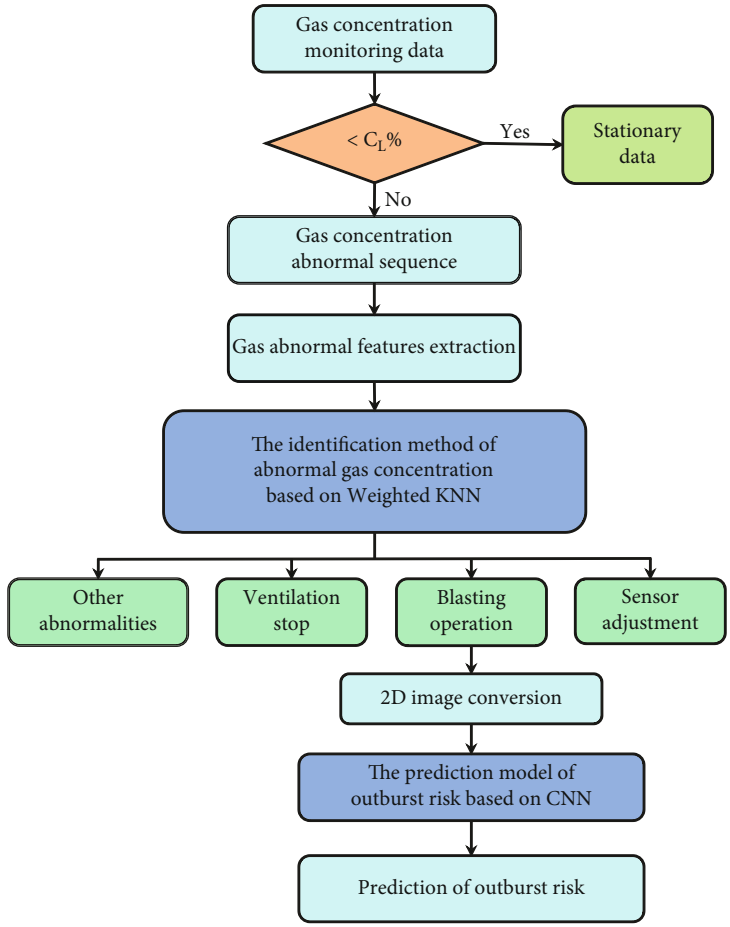

Figure 4: The process of gas abnormal identification and outburst risk prediction.

larger weight to the point closer to the point to be classified. Each feature of the new sample is compared with the corresponding feature in the training sample set, and the classification label of the most similar data of the sample is obtained through this algorithm. CNN is a special type of deep feedforward neural network containing convolutional computation [33], which is mainly composed of the input layer, convolution layer, pooling layer, activation layer, full connection layer, and output layer [34]. The convolution layer is used to extract the features of input layer, and pooling layer is used for information filtering and feature selection.

In the training process of CNN, the distribution of input data is different, and some different values will be generated after matrix multiplication with weight. The slight change of the difference values will affect the back layer network, lead to gradient divergence, and reduce the generalization ability and training speed of the network. To solve this problem, a batch normalization (BN) method is proposed [35].

The shape of underground gas signal is affected by many factors, and the most important one is the gas content in coal seam, which is an important basis for judging the dangerous of coal and gas outburst. If an abnormal gas concentration is caused by an accident rather than coal seam gas content, it does not indicate an increased risk of coal and gas outburst. Therefore, before judging the risk of coal and gas outburst, it is necessary to eliminate the invalid data of gas anomaly.

In our work, a comprehensive technology is put forward. When it is applied, the "weighted KNN" technology is used to identify valid data, and the "CNN" technology is used to predict the danger. The above two technologies can be used simultaneously to make the prediction results more accurate.

3. Prediction of Coal and Gas Outburst Risk by Gas after Blasting

3.1. Correlation Analysis between Gas Concentration after Blasting and K_1. During coal roadway excavation, the K_1 value will be tested and obtained regularly. In this section, the correlation between the gas emission characteristics after blasting and K_1 value is analyzed to explain the rationality of predicting outburst risk by using gas emission characteristics after blasting. The K_1 value is the gas desorption amount of one gram of coal sample within one minute after collection, and the unit is $cm^3/g{\cdot}min^{1/2}$. The higher the K_1 value is, the higher the risk of coal and gas outburst is [36, 37].

In order to compare and analyze the specific change characteristics of gas concentration after blasting under different K_1 values, for each identified blasting event, the gas

concentration curve is divided into two stages: The first stage is the straight-line rising stage, in which the gas concentration shows a straight-line upward trend, and the gas emission is mainly affected by the falling coal and coal wall. The second stage is the slow decline stage, in which the gas concentration shows a slow decline trend, and the gas emission is mainly affected by the coal wall. Starting from the blasting time, a gas concentration value is extracted every 10 s in the first stage and every 5 min in the second stage. In order to reduce accidental error, for the blasting events with the same K_1 value, take the average value of gas concentration at the same interval after blasting. The variation characteristics of the average gas concentration after blasting with time Δt under different K_1 values in the two stages are shown in Figure 5.

It can be seen from Figure 5(a) that in the first stage (within 2 min after blasting), the gas concentration curve presents the same characteristics of straight-line rising, and the larger K_1 value is, the larger the growth rate and peak value of gas concentration are. In the second stage, as shown in Figure 5(b), the gas concentration shows the same logarithmic decay characteristic with time, and the larger K_1 value is, the faster the decay rate of gas concentration is, and the longer the time required to recover to a stable value is.

In order to quantitatively analyze the correlation between the growth rate, peak value, and decay rate of gas concentration after blasting and K_1 value, the correlation analysis is carried out. The results are shown in Table 2.

It can be seen from Table 2 that the correlation coefficients between the growth rate, peak value, and decay rate of gas concentration after blasting and K_1 value are 0.85, 0.92, and 0.79, respectively, which are strongly correlated with K_1 value. At the same time, there are also strong correlations between the growth rate, peak value, and decay rate of gas concentration. Therefore, it is reasonable to predict the outburst risk in the front of blasting working face by using gas emission characteristics after blasting.

3.2. Input and Output Layer of CNN. The convolutional neural network is a model applied to extract deep image features, with the characteristics of local connection, weight sharing, and pooling. It overcomes the disadvantages of high cost, low precision, and non-generalization of traditional manual feature extraction. The original gas concentration time series is transformed into two-dimensional images to provide image data input for CNN. As shown in Figure 6, the gas concentration data identified after blasting is mapped into an RGB image with a size of $120 \times 120 \times 3$ according to the time sequence and numerical size. which is used as the input layer of CNN. Compared with the gas concentration time series as the input layer, this conversion enriches the gas concentration characteristics after blasting more obvious.

The purpose of applying CNN is to predict the risk of outburst, but there is no unified and fixed index to reflect outburst. According to the relevant research of Han [38], the outburst prediction indexes adopted in the area where the Jinjia coal mine is located are mainly the value of gas desorption index K_1 and Δh_2 of drilling cuttings, the volume of drilling cuttings S, and the initial velocity q of drilling gas emission. After years of practical experience in outburst prediction in the test mining area, the sensitive index of outburst prediction is determined as K_1 value. Therefore, the K_1 value is used as the index to reflect the outburst risk in this paper. For each blasting image, the K_1 value is used as the output layer to reflect the outburst risk in the front of the driving working face. For blasting images processed by gas concentration curve, compare the blasting time with the information recorded by K_1 value, and each blasting image corresponds to the corresponding K_1 value. 16 groups of samples are randomly selected from all image samples. The blasting images with different K_1 values are shown in Figure 7.

It can be seen from Figure 7 that there are obvious differences in blasting images with different K_1 values. The larger the K_1 value corresponding to the image, the higher the overall brightness of the image, that is, the larger the gas concentration value corresponding to each stage, which is also consistent with the relationship between gas emission characteristics after blasting and K_1 value in Section 4.1.

3.3. Outburst Risk Prediction Model. The normalized data of the blasting image is used as the input layer of CNN. CNN is composed of a multilayer convolution filter and subsampling filter alternately, and the image is convolved with multiple convolution kernels. After convolution, the image features are uniformly processed by BN, and the pooling layer adopts max pooling to reduce dimensions. After the blasting image goes through the process of convolution → pooling → convolution → pooling → convolution → pooling → convolution, local connection and weight sharing are adopted to filter out process noise and interference information to obtain high-level abstract expression of process data. The dropout layer is applied to discard neurons from the network with a probability of 20% to prevent CNN overfitting.

Different characteristics are learned in a supervised manner to predict the outburst risk. The parameters of the outburst risk prediction model based on CNN are shown in Table 3, and the prediction model establishment process is shown in Figure 8.

Coal and gas outburst disaster is affected by many factors, such as stress, coal mechanical properties, and gas. Any factor can play a role in gas outburst. This paper takes gas as the main research object. By analyzing the law of characteristic parameters of gas data, we can find out what kind of gas concentration tend after blasting corresponds to coal and gas outburst risk, so as to realize real-time monitoring and identification of danger.

4. Field Applications

4.1. Gas Concentration Data Collection. In our work, the measured location of this work is located in Jinjia coal mine in Guizhou Province, China. The average thickness of the coal seam is 1.2 m, and the average f value of the coal seam firmness coefficient is 0.5~0.6. The average buried depth is 320 m. There are ridges and valleys on the surface.

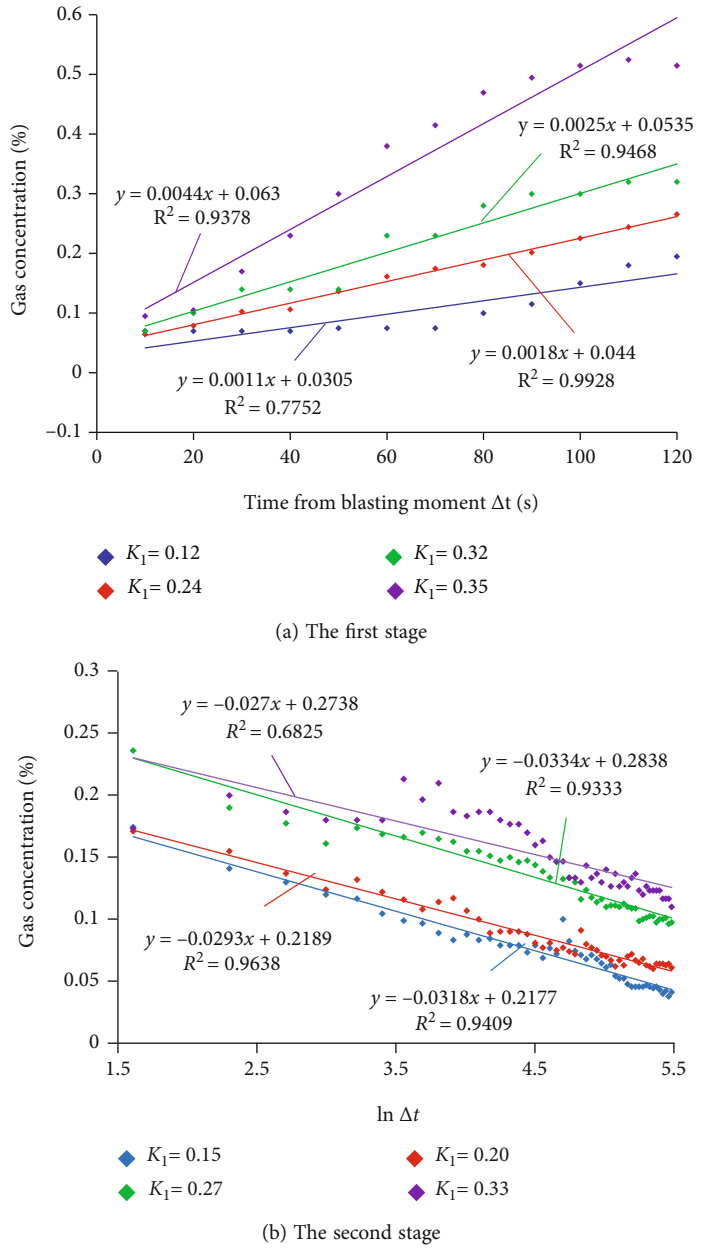

Figure 5: Variation characteristics of gas concentration after blasting under different K_1 values.

Table 2: Correlation between the growth rate, peak value, and decay rate of gas concentration and K_1 value.

Correlation coefficient	K_1 value ($cm^3/g{\cdot}min^{1/2}$)	Growth rate ($\%/s \times 10^{-3}$)	Peak value/%	Decay rate ($\% \times 10^{-2}$)
K_1 value	1.00	0.85	0.92	0.79
Growth rate	0.85	1.00	0.87	0.72
Peak value	0.92	0.87	1.00	0.84
Decay rate	0.79	0.72	0.84	1.00

Therefore, the buried depth of coal seams in different areas varies greatly. The buried depth at the upper corner of the cutting hole of the working face is the shallowest.

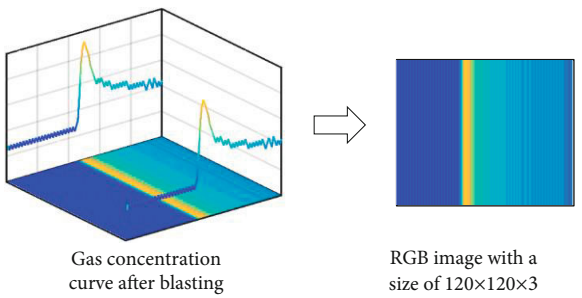

Figure 6: Gas concentration data after blasting is mapped into an RGB image.

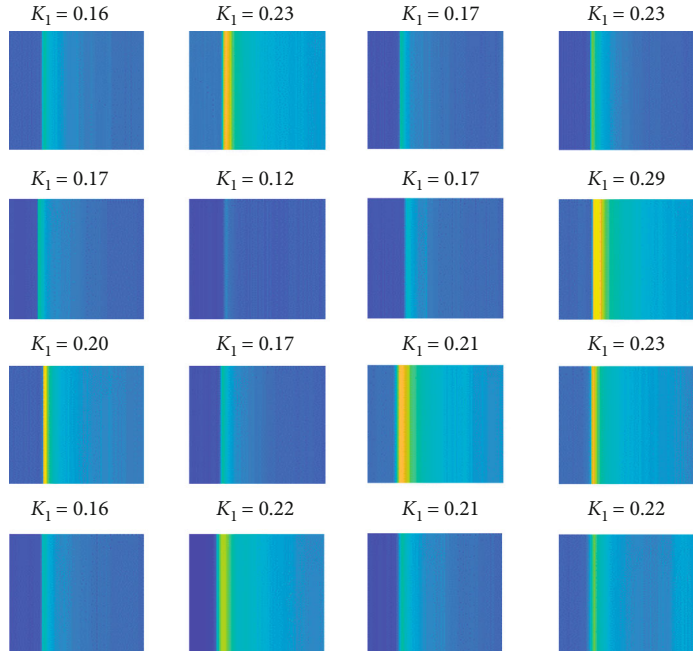

Figure 7: Gas concentration images after blasting with different K_1 values.

Table 3: The parameters of the outburst risk prediction model based on CNN.

Convolution parameters	Value/type	Pooling parameters	Value/type
Convolution kernel size	$f = 5 \times 5$	Pooling kernel size	$f = 2 \times 2$
Convolution step length	$s_0 = 1$	Pooling step length	$s_0 = 2$
Filling style	Same padding	Filling style	—
Number of filling layers	$p = 2$	Number of filling layers	$p = 0$
Activation function	ReLU	Pooling style	Max pooling

In this paper, we select the historical data stored by the gas and wind speed sensor of a station in the safety monitoring system of 1138 and 11224 transportation roadways of Jinjia coal mine in China. The sampling time of 1138 and 11224 transportation roadways is January 1, 2019, to April 30, 2019, and August 1, 2017, to December 31, 2017. The gas data sample set of 1138 transportation roadway is used for model training, and that of 11224 transportation roadway is used for model verification. Jinjia coal mine is a coal and gas outburst mine. The average gas content of 3# coal seam of 1138 transportation roadway and 22# coal seam of 11224 transportation roadway are 17.55 m^3/t and 10.79 m^3/t, respectively, and the average gas pressure is 0.97 MPa and 1.80 MPa, respectively. The gas content and the gas pressure are all high. It is easy to cause local gas emissions and coal and gas outburst during roadway driving.

Gas sensors T_1, T_2, and T_3 should be arranged in the driving roadway to monitor the gas concentration in real time. The layout of T_1, T_2, and T_3 is shown in Figure 9. It can be seen from Figure 9 that the gas sensor T_1 is closest to the blasting driving face and can reflect the change of gas concentration in front of the blasting driving face in real time. During the field test, T_1 sensor is located 5 m in front of the excavation. Therefore, the monitoring data of gas sensor T_1 is used for analysis in this paper.

In the Jinjia coal mine, gas monitoring system is a system used to monitor gas concentration and change to prevent gas accidents. The gas monitoring system is mainly composed of monitoring host, computer network, monitoring software, transmission interface and transmission channel, underground data acquisition substation, various sensors, and actuators. These systems work together to form a complete gas monitoring system. The gas monitoring system monitors and records the gas concentration at the monitoring site in real time and visually displays the gas concentration monitoring curve on the monitoring screen. The gas concentration data in the paper is obtained from the gas monitoring system.

4.2. Field Application of Identification Method. The gas concentration data of 1138 transportation roadway are analyzed to obtain the gas concentration abnormal sequence with the peak value of no less than 0.15%, 10 min before the peak and 30 min after the peak. The 12 features of each gas concentration abnormal sequence are calculated, and the deviation standardization method is used to map the feature data

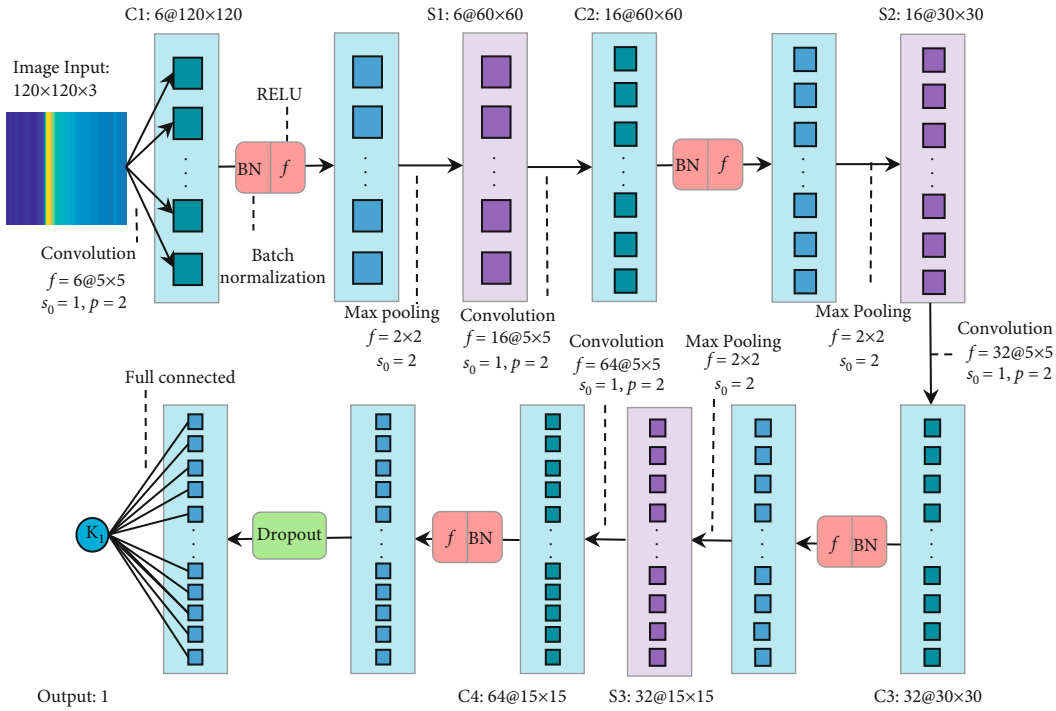

Figure 8: Prediction model of outburst risk based on CNN.

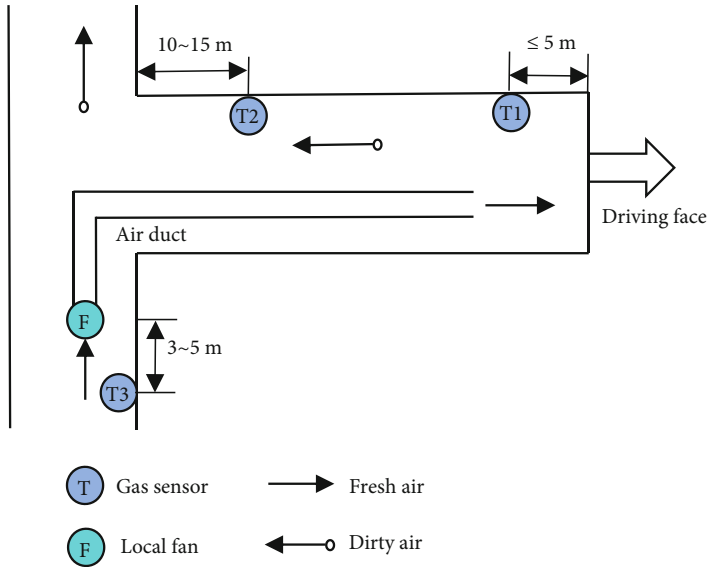

Figure 9: Layout of gas sensors in blasting driving face.

between [0,1], so as to eliminate the dimensional influence between features.

The feature data set and corresponding cause label constitute the sample data set. The first 80% of the sample data set is divided into the training set and the last 20% into the test set. The training and test sets are separately input into the weighted KNN classifier for continuous training and optimization to verify the model. In the training process, the Euclidean distance is used to reflect the distance between samples, and the Gaussian function is used to increase the weight. The value of k is 10, which means that the 10 samples with the smallest distance are selected for comparison. The model training is verified by 5-fold cross validation. The confusion matrix of the identification results is shown in Figure 10.

As the data features of the four abnormal sequences interact and overlap each other in space, the weighted KNN has a certain degree of "cause confusion" in identifying each abnormal cause, that is, a small number of "misclassification" phenomena occur in each abnormal cause. It is easy to classify ventilation stops as a blasting operation or other abnormalities, especially in identifying ventilation stops. However, most samples can be correctly classified into the corresponding causes.

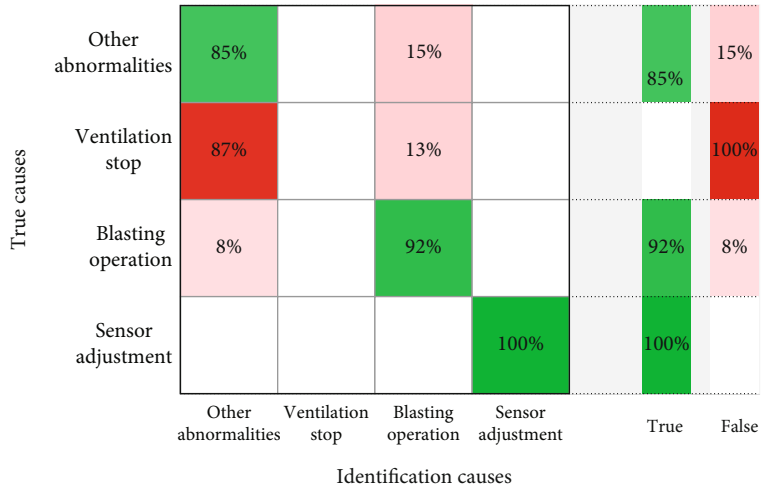

Figure 10: The confusion matrix of the identification results.

The confusion matrix reflects the advantages and disadvantages of weighted KNN in identifying the abnormal gas concentration. The ROC (receiver operating characteristic) curve can be used to evaluate the classification performance of the method as a whole. The ROC curve is the line of each point with a false-positive rate as abscissa and a true-positive rate as ordinate. AUC (area under curve) represents the area under the ROC curve, between 0.1 and 1, which can measure the generalization performance of the method. Figure 11 shows the ROC curve of the weighted KNN. The current classifier performance is (0.12,0.85), representing an 85% true-positive rate and a 12% false-positive rate (Figure 11). In other words, the probability that weighted KNN correctly judges the cause of abnormal gas signal is 85% and the probability of error is 12%. $AUC = 0.91$, and $0.5 < AUC < 1$; therefore, the proposed weighted KNN method is superior to random guess and has a certain identification value.

The weighted KNN method trained by the gas concentration data of 1138 transportation roadway is applied to 11224 transportation roadway, and the abnormal gas concentration is marked differently according to the different causes. Typical identification results are shown in Figure 12.

It can be seen from Figure 12 that the identification results by the proposed method are generally consistent with the judgment results of manually viewed waveform curves. In particular, the identification of blasting operation events is more accurate, which lays a foundation for the prediction of outburst risk by using the characteristics of gas emission after blasting.

4.3. Field Application of Prediction Model. The blasting operation events identified in 1138 transportation roadway are applied to establish an outburst risk prediction model. The blasting image and K_1 value are mapped to form a sample data set. The first 80% of the sample data set is divided into the training set, and the last 20% into the test set, which is input into CNN for continuous training and optimization. The trained CNN is applied to 11224 transportation roadway, and the prediction results are analyzed and evaluated

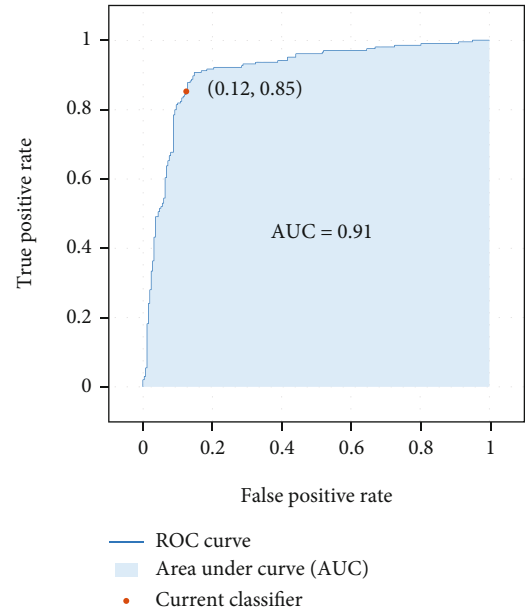

Figure 11: ROC curve of the identification results.

in combination with small gas dynamic performances such as jet holes and outburst.

The jet hole is a phenomenon of dynamic manifestation; coal and gas are ejected from the borehole during the drilling of coal seam with risk of coal and gas outburst, especially in soft coal seams under high in situ stress, high gas pressure, and gas content. The jet hole can be considered micro coal and gas outburst [17]. According to the Rules for the Prevention and Control of Coal and Gas Outburst [37], the outburst mine should determine the sensitive indexes and critical values for the driving working face prediction through experiments according to the characteristics and conditions of each coal seam and serve as the main basis for judging the outburst risk of the driving working face. In the practice of outburst prediction in Jinjia coal mine for many years, the K_1 value is taken as the sensitive index of outburst prediction. According to the Rules for the

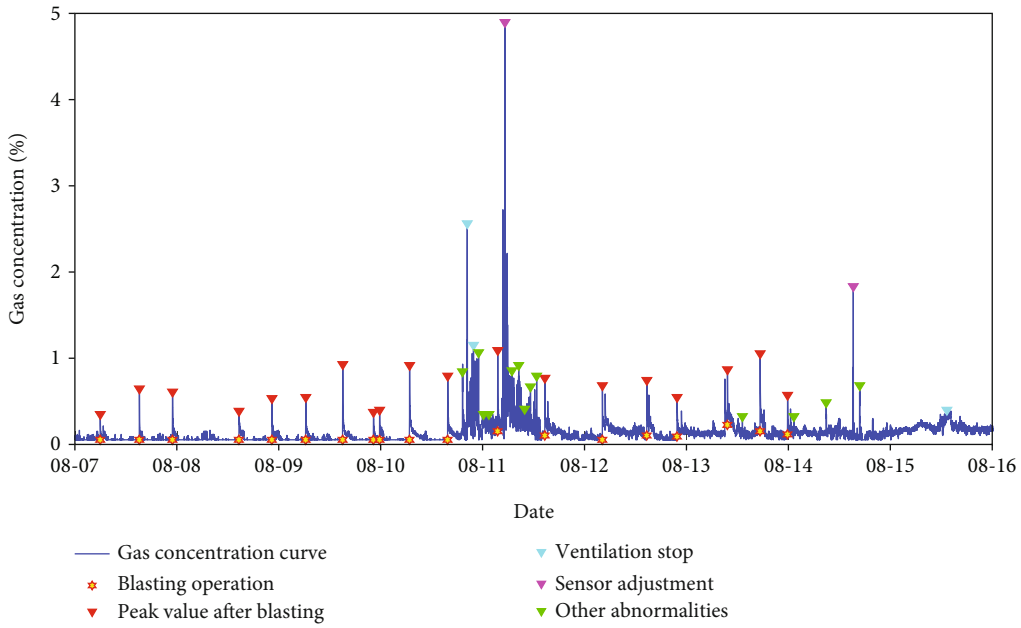

(a) Identification results of abnormal gas concentration in August 2017

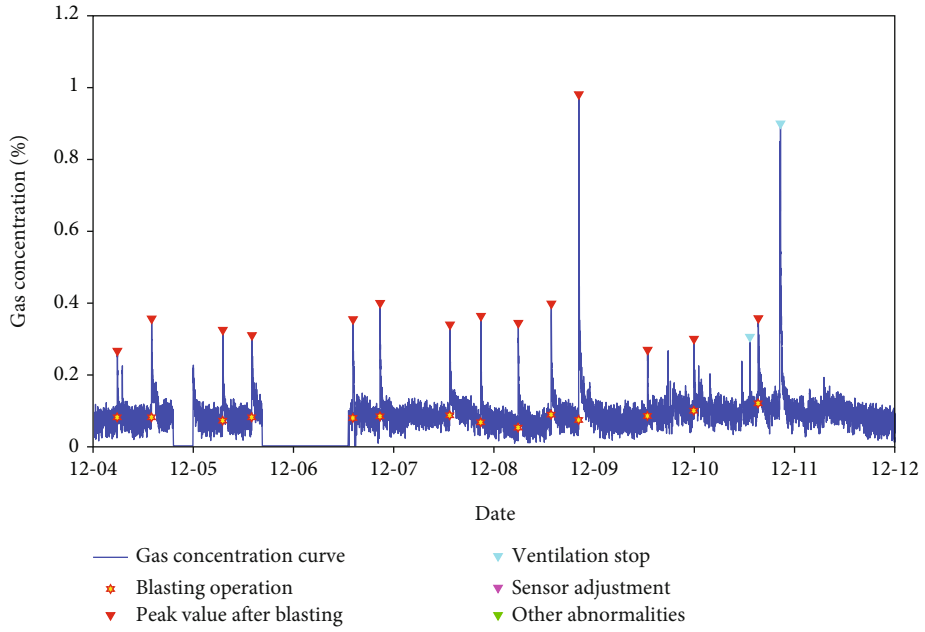

(b) Identification results of abnormal gas concentration in December 2017

Figure 12: Identification results in 11224 transportation roadway.

Prevention and Control of Coal and Gas Outburst, the predictions are carried out in strict reference to the index critical value of 0.5 $cm^3/g{\cdot}min^{1/2}$. That is, when the measured K_1 value exceeds 0.5 $cm^3/g{\cdot}min^{1/2}$, there will be an outburst risk in front of the blasting driving working face, and relevant outburst prevention measures should be taken.

Based on the characteristics identification results of abnormal gas concentration after blasting operations in 11224 transport roadway from August to December 2017, the risk prediction model of coal and gas outburst is applied to predict the K_1 value of each identified blasting event. According to the prediction results of K_1 value and its critical value, 28 times of jet holes and 1 small outburst event in the front of 11224 working face are predicted successfully. Figure 13 selects the gas concentration monitoring curves and corresponding events of 11224 transportation roadway in August and December 2017 to analyze the outburst risk prediction results.

As shown in Figure 13(a), the predicted K_1 values are 0.51737, 0.52890, 0.57401, and 0.58149, respectively, in the four blasting events from August 9 to 10, all exceeding the K_1 critical value of 0.5. The jet holes event occurred during drilling at the third shift on August 10, while the measured K_1 values on August 8 to 10 were all 0.27, which did not

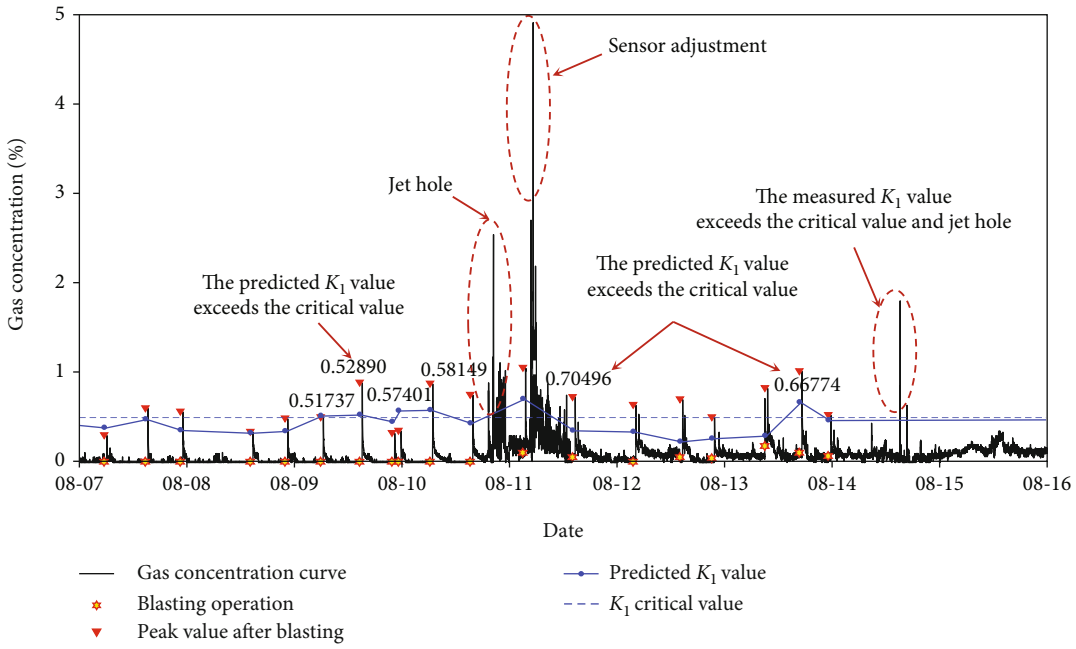

(a) Jet holes events in August 2017

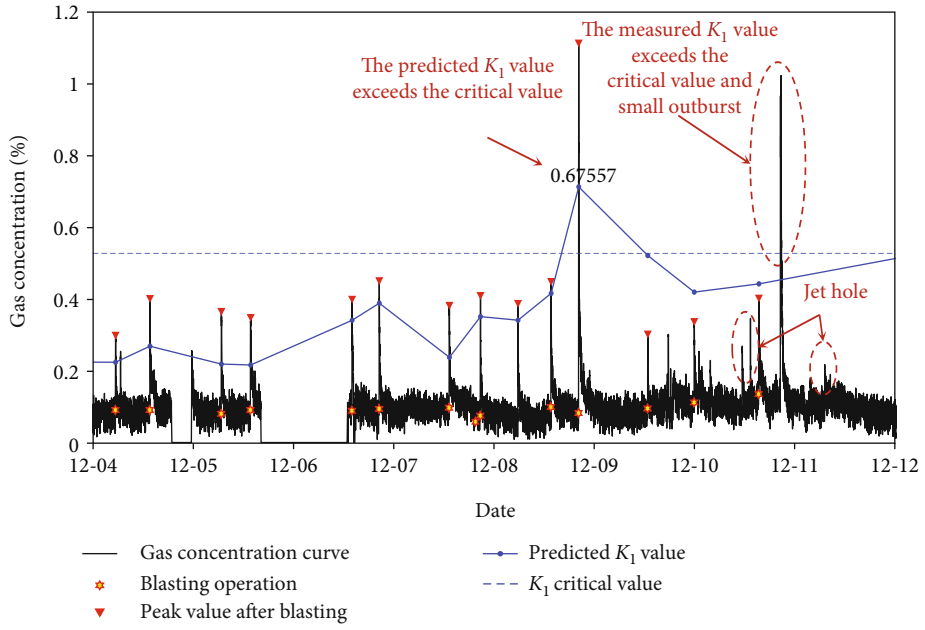

(b) Jet holes and outburst events in December 2017

Figure 13: Analysis of outburst risk prediction results.

exceed the K_1 critical value. In a blasting event of the first shift on August 11, the predicted K_1 value is 0.70496, exceeding the K_1 critical value of 0.5. However, there were no outburst events such as jet holes in the following three days, which is a failed prediction. In the third shift blasting event on August 13, the predicted K_1 value is 0.66774, exceeding the K_1 critical value of 0.5. On August 15, the measured K_1 value was 0.52, and a jet hole occurred during drilling.

As shown in Figure 13(b), on December 8, the blasting operation was carried out three times in front of the blasting driving face 11224. The predicted K_1 value of the third blasting event is 0.67557, exceeding the K_1 critical value of 0.5. From December 9 to 11, the jet holes event occurred four times, and the measured K_1value on December 10 was 0.52, accompanied by one small outburst event.

4.4. Evaluation of Prediction Results. From August to December 2017, the jet holes event occurred for 32 times in the 11224 transportation roadway. See Table 4 for the specific time of jet holes.

Table 4: Jet holes events in 11224 transportation roadway.

Number	Date	Shift	Number	Date	Shift	Number	Date	Shift
1	2017.08.10	3rd	12	2017.9.15	1st	23	2017.12.11	1st
2	2017.08.15	3rd	13	2017.9.16	1st	24	2017.12.13	1st
3	2017.08.27	3rd	14	2017.9.23	3rd	25	2017.12.13	1st
4	2017.08.27	3rd	15	2017.9.23	3rd	26	2017.12.14	1st
5	2017.09.01	3rd	16	2017.9.23	1st	27	2017.12.14	3rd
6	2017.09.08	3rd	17	2017.10.15	1st	28	2017.12.16	3rd
7	2017.09.09	2nd	18	2017.10.25	1st	29	2017.12.19	1st
8	2017.09.13	2nd	19	2017.10.31	1st	30	2017.12.20	1st
9	2017.09.13	1st	20	2017.12.09	3rd	31	2017.12.20	2nd
10	2017.09.13	1st	21	2017.12.10	3rd	32	2017.12.21	2nd
11	2017.09.14	1st	22	2017.12.10	1st	—	—	—

The predicted K_1 value exceeds the critical value 18 times, applied the established outburst risk prediction model. The prediction period is set as 3 days. That is, if there are jet holes or other gas dynamic phenomena within 3 days after the predicted K_1 value exceeds the critical value, the prediction is considered to success. Among the 18 times exceeding the critical value, 16 times of prediction are successful, and 2 times are failed. Among the 32 times jet holes events, 28 times are predicted accurately, and 4 times are missed. In order to objectively evaluate the prediction model and comprehensively consider the impact of accurate predictions, failed predictions, and missing predictions, the R -score method is used to evaluate the outburst risk prediction results. The larger the R is, the better the effect is. Prediction efficiency R [20, 39] is defined as

$$R = \frac{n_1^1}{N_1} - \frac{n_0^1}{N_0}, \tag{4}$$

where n_1^1 , n_0^1 , N_1, and N_0 are, respectively, the number of jet holes accurate predictions, failed predictions, occurrences, and out of the critical value times, and their values are 28, 2, 32, and 18, respectively. According to Equation (4), the prediction efficiency R is 76.39%.

5. Discussion about Abnormal Gas Emission during the Evolution of Coal and Gas Outburst

The occurrence of coal and gas outburst is essentially the instability and failure of gas bearing coal. In the process of coal roadway driving, on the one hand, the change of coal seam stress state and distribution changes the occurrence state of gas; on the other hand, mining activities change the pore structure of coal seam, resulting in the change of gas flow mode in coal seam. The change of coal structure in front of the blasting driving face during coal and gas outburst induced by coal roadway driving is shown in Figure 14.

As shown in Figure 14(a), at the beginning of roadway driving, the coal seam is in a stable state, and the coal structure changes little. With the increase of driving distance, the impact of mining activities on the structure of coal and rock mass is gradually significant. However, according to the simulation results above, when the driving distance reaches 3.0 m as shown in Figure 14(b), the coal is still stable, and the coal structure has not changed significantly. When the roadway driving distance reaches 3.4 m as shown in Figure 14(c), macro cracks appear at about 0.5 m in front of the driving face, and fracture zones are formed and initially connected, and the coal gas can flow to the roadway through the fracture zone. When the driving distance reaches 4 m, a large amount of gas gushes out from the deep coal seam, and the high-pressure gas flow quickly throws the coal body from the coal seam to the roadway, forming a large-scale dynamic disaster of coal and gas outburst.

In the process of coal and gas outburst disaster illustrated in Figure 14, it has been accompanied by the outward gas emission of coal seam. If the mining activity does not significantly impact on the coal structure in front of the blasting driving face, the evolution of the disaster is in the state of Figure 14(a) or Figure 14(b), and gas emission is relatively stable. At this time, the coal seam is safe and can be excavated normally. If the mining activity has a significant impact on the coal structure in front of the blasting driving face, the evolution of the disaster is in the state of Figure 14(c), and gas emission will be different from normal. At this time, the coal seam is at risk, and measures should be taken to eliminate the outburst risk.

According to the simulation results of the evolution process of coal and gas outburst, during coal roadway excavation, the relationship between gas emission and coal and gas outburst danger is very close, and different risks would show different characteristics of gas emission, which provides a theoretical basis for the technical application of this paper.

Figure 14 also shows that the process of coal and gas outburst is very complex, and there will be false warnings and missing alarms only by the threshold early warning method. It is necessary to predict outburst risk according to the gas emission trend.

The prediction method based on gas characteristics after blasting has good applicability in coal and gas outburst risk early warning process of blasting driving face. In addition,

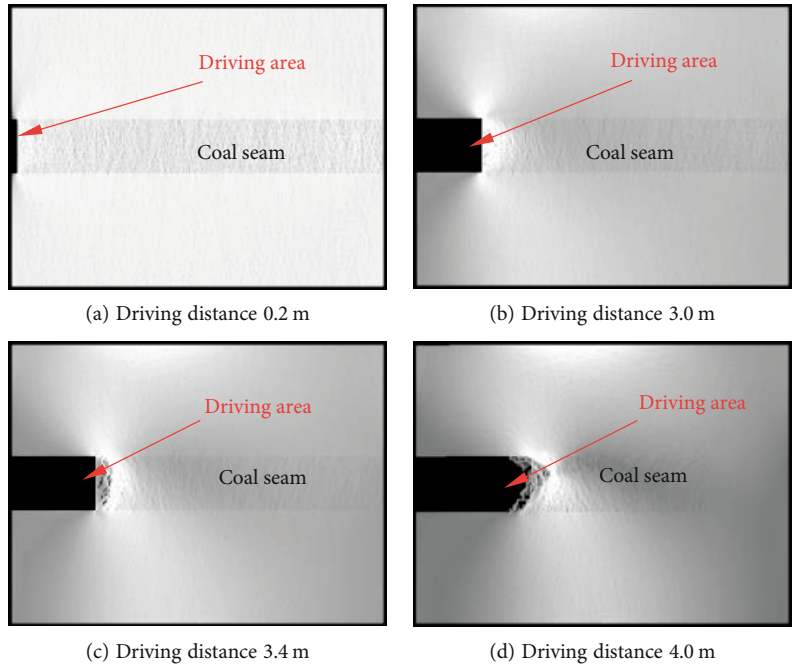

(a) Driving distance 0.2 m (b) Driving distance 3.0 m

(c) Driving distance 3.4 m (d) Driving distance 4.0 m

Figure 14: Evolution process of coal and gas outburst during coal roadway driving [40].

the method proposed in this paper to predict disaster risk through in-depth analysis of common signal characteristics has good applicability for complex coal and rock power disaster monitoring and early warning.

6. Conclusions

At present, there is a lack of reliable real-time prediction technology for the risk of coal and gas outburst in blasting faces. An outburst risk prediction method based on the characteristics of gas emission after blasting is proposed to solve this problem, which has achieved good results in application. The main conclusions are as follows:

(1) The prediction method of coal and gas outburst risk can be well applied in blasting driving face; firstly, the gas concentration anomaly is identified based on Weighted KNN, and then the outburst risk is predicted based on CNN. This method can be used to supplement the existing outburst prediction methods and assist the traditional prediction indexes in the dynamic and continuous prediction of outburst risk

(2) The accuracy of the identification method of abnormal gas concentration based on the weighted KNN proposed in this study is 86.1%, of which the identification accuracy of blasting operation is 92%. It provides a new idea for determining the causes of gas concentration exceeding the limit in driving face

(3) There are strong correlations between the growth rate, peak value, and decay rate of gas concentration after blasting and K_1 value, and the maximum correlation coefficient is 0.92. The blasting images with different K_1 values are obviously different. The larger the K_1 value corresponding to the image is, the higher the overall brightness of the blasting image is, the larger the corresponding gas concentration value is

(4) The prediction model established in this study by inputting blasting images to CNN achieves a good predictive effect in coal and gas outburst prediction. 28 times of jet holes and 1 small outburst event in the front of 11224 working face of Jinjia coal mine are predicted successfully, and the prediction efficiency of the model is 76.39%

This technology establishes the relationship between the change characteristics of gas concentration after blasting and the risk of coal seam outburst, which is significant to improving the prediction accuracy of coal and gas outburst.

Data Availability

The raw/processed data required to reproduce these findings cannot be shared at this time as the data also forms part of an ongoing study.

Conflicts of Interest

The authors declare no competing financial interests or personal relationships that could have appeared to influence the work in this paper.

Acknowledgments

This work was supported by the National Natural Science Foundation of China (Grant Nos. 52004016, 52174162, and

51904019), the State Key Laboratory Cultivation Base for Gas Geology and Gas Control (Henan Polytechnic University) (Grant No. WS2020B01), the Open Fund Project of Shaanxi Key Laboratory of Prevention and Control Technology for Coal Mine Water Hazard (2021SKMS05), the Major Science and Technology Innovation Project of Shandong Province (2019SDZY01), the Planning Textbook Project of USTB (Grant No. JC2021JY007), and the Science and Technology Support Plan Project of Guizhou Province ([2021]515).

References

[1] Y. Ma, B. Nie, X. He, X. Li, J. Meng, and D. Song, "Mechanism investigation on coal and gas outburst: An overview," *International Journal of Minerals Metallurgy and Materials*, vol. 27, no. 7, pp. 872–887, 2020.

[2] L. Yuan, Y. Jiang, X. He, L. Dou, and H. Li, "Research progress of precise risk accurate identification and monitoring early warning on typical dynamic disasters in coal mine," *Journal of China Coal Society*, vol. 43, no. 2, pp. 306–318, 2018.

[3] X. Li, Z. Cao, and Y. Xu, "Characteristics and trends of coal mine safety development," *Energy Sources, Part A: Recovery, Utilization, and Environmental Effects*, vol. 2020, pp. 1–14, 2020.

[4] L. Qiu, Z. Liu, E. Wang, X. He, J. Feng, and B. Li, "Early-warning of rock burst in coal mine by low-frequency electromagnetic radiation," *Engineering Geology*, vol. 279, article 105755, 2020.

[5] L. Yuan, "Strategic thinking of simultaneous exploitation of coal and gas in deep mining," *Journal of China Coal Society*, vol. 41, no. 1, pp. 1–6, 2016.

[6] G. Fu, X. Xie, Q. Jia, W. Tong, and Y. Ge, "Accidents analysis and prevention of coal and gas outburst: understanding human errors in accidents," *Process Safety and Environmental Protection*, vol. 134, pp. 1–23, 2020.

[7] S. Liu, X. Li, D. Wang, and D. Zhang, "Experimental study on temperature response of different ranks of coal to liquid nitrogen soaking," *Natural Resources Research*, vol. 32, no. 2, pp. 1467–1480, 2021.

[8] D. Fernandez, N. Gonzalez, F. Alvarez, and G. Lopez, "Analysis of gas-dynamic phenomenon in underground coal mines in the central basin of Asturias (Spain)," *Engineering Failure Analysis*, vol. 34, no. Si, pp. 464–477, 2013.

[9] J. Feng, E. Wang, H. Ding, Q. Huang, and X. Chen, "Deterministic seismic hazard assessment of coal fractures in underground coal mine: a case study," *Soil Dynamics and Earthquake Engineering*, vol. 129, pp. 105921–105931, 2020.

[10] X. Kong, S. Li, E. Wang et al., "Experimental and numerical investigations on dynamic mechanical responses and failure process of gas-bearing coal under impact load," *Soil Dynamics and Earthquake Engineering*, vol. 142, p. 106579, 2021.

[11] C. Jiang, L. Xu, X. Li et al., "Identification model and indicator of outburst-prone coal seams," *Rock Mechanics and Rock Engineering*, vol. 48, no. 1, pp. 409–415, 2015.

[12] X. Li, S. Chen, Z. Li, and E. Wang, "Rockburst mechanism in coal rock with structural surface and the microseismic (MS) and electromagnetic radiation (EMR) response," *Engineering Failure Analysis*, vol. 124, no. 6, p. 105396, 2021.

[13] W. Cheng, X. Zhang, and F. Wu, *Theory and Technology of Regional Prediction of Coal and Gas Outburst*, Coal Industry Press, Beijing, 2005.

[14] S. Yang, J. Tang, S. Zhao, and H. Fu, "Early warning on coal and gas outburst with dynamic indexes of gas emission," *Disaster Advances*, vol. 3, no. 4, pp. 403–406, 2010.

[15] Q. Qi, Y. Pan, H. Li et al., "Theoretical basis and key technology of prevention and control of coal-rock dynamic disasters in deep coal mining," *Journal of China Coal Society*, vol. 45, no. 5, pp. 1567–1584, 2020.

[16] J. Mou, H. Liu, Y. Zou, and Q. Li, "A new method to determine the sensitivity of coal and gas outburst prediction index," *Arabian Journal of Geosciences*, vol. 13, no. 12, p. 465, 2020.

[17] C. Wang, S. Yang, X. Li, D. Yang, and C. Jiang, "The correlation between dynamic phenomena of boreholes for outburst prediction and outburst risks during coal roadways driving," *Fuel*, vol. 231, pp. 307–316, 2018.

[18] J. Li, Q. Hu, M. Yu, X. Li, and H. Yang, "Acoustic emission monitoring technology for coal and gas outburst," *Energy Science & Engineering*, vol. 7, no. 2, pp. 443–456, 2019.

[19] H. Wang, D. Song, Z. Li, H. He, S. Lan, and H. Guo, "Acoustic emission characteristics of coal failure using automatic speech recognition methodology analysis," *International Journal of Rock Mechanics and Mining Sciences*, vol. 27, no. 12, article e2639, 2020.

[20] X. Tian, Z. Li, D. Song et al., "Study on microseismic precursors and early warning methods of rockbursts in a working face," *Chinese Journal of Rock Mechanics and Engineering*, vol. 39, no. 12, pp. 2471–2482, 2020.

[21] A. Wang, D. Song, X. He, Q. Lou, and Y. Zhao, "Investigation of coal and gas outburst risk by microseismic monitoring," *PLoS One*, vol. 14, no. 5, article e0216464, 2019.

[22] L. Qiu, D. Song, Z. Li, B. Liu, and J. Liu, "Research on AE and EMR response law of the driving face passing through the fault," *Safety Science*, vol. 117, pp. 184–193, 2019.

[23] L. Qiu, Y. Zhu, D. Song et al., "Study on the Nonlinear Characteristics of EMR and AE during Coal Splitting Tests," *Minerals*, vol. 12, no. 2, p. 108, 2022.

[24] L. Chen, E. Wang, J. Feng, X. Wang, and X. Li, "Hazard prediction of coal and gas outburst based on fisher discriminant analysis," *Geomechanics and Engineering*, vol. 13, no. 5, pp. 861–879, 2017.

[25] Y. Wu, R. Gao, and J. Yang, "Prediction of coal and gas outburst: a method based on the BP neural network optimized by GASA," *Process Safety and Environmental Protection*, vol. 133, pp. 64–72, 2020.

[26] Z. Li, E. Wang, J. Ou, and Z. Liu, "Hazard evaluation of coal and gas outbursts in a coal-mine roadway based on logistic regression model," *International Journal of Rock Mechanics and Mining Sciences*, vol. 80, pp. 185–195, 2015.

[27] W. Wang, H. Wang, B. Zhang, S. Wang, and W. Xing, "Coal and gas outburst prediction model based on extension theory and its application," *Process Safety and Environmental Protection*, vol. 154, pp. 329–337, 2021.

[28] C. Zhang, E. Wang, and S. Peng, "Research on temperature variation during coal and gas outbursts: implications for outburst prediction in coal mines," *Sensors*, vol. 20, no. 19, p. 5526, 2020.

[29] J. Wei, P. Cui, Z. Chen et al., "Experimental study on radon exhalation characteristics of coal samples under varying gas pressures," *Results in Physics*, vol. 10, pp. 1006–1014, 2018.

[30] B. Zhou, S. Yang, C. Wang, J. Cai, Q. Xu, and N. Sang, "Experimental study on the influence of coal oxidation on coal and gas outburst during invasion of magmatic rocks into coal

seams," *Process Safety and Environmental Protection*, vol. 124, pp. 213–222, 2019.

[31] X. Li and W. Zhou, "The risk forecast of coal and gas outburst on blasting-working- face by the method of gas peak-to-valley ratio," *Journal of China Coal Society*, vol. 37, no. 1, pp. 104–108, 2012.

[32] H. Peter, *Machine Learning*, Posts and Telecom Press, Beijing, 2013.

[33] I. Goodfellow, Y. Bengio, and A. Courville, *Deep Learning*, MIT Press, Cambridge, MA, 2016, http://www.deeplearningbook.org/.

[34] M. Sarigul, B. Ozyildirim, and M. Avci, "Differential convolutional neural network," *Neural Networks*, vol. 116, pp. 279–287, 2019.

[35] I. Sergey and S. Christian, "Batch normalization: accelerating deep network training by reducing internal covariate shift," *International Conference on Machine Learning*, vol. 37, pp. 448–456, 2015.

[36] L. Shu, N. Zhu, J. Chen, S. An, and H. Zhang, "Theoretical method and technology of precision identification for coal and gas outburst hazard," *Journal of China Coal Society*, vol. 45, no. 5, pp. 1614–1625, 2020.

[37] National Coal Mine Safety Admin, *Rules for the Prevention and Control of Coal and Gas Outburst*, China Coal Industry Publishing House, Beijing, 2019.

[38] Z. Han, S. Zhang, X. Heng, X. Xu, and X. Li, "Study on technical system of coal and gas outburst prevention and control in Guizhou coal mines," *Safety in Coal Mines*, vol. 48, no. 11, pp. 9–12, 2017.

[39] Y. Xia, L. Kang, Q. Qi et al., "Five indexes of microseismic and their application in rock burst forecastion," *Journal of China Coal Society*, vol. 35, no. 12, pp. 2011–2016, 2010.

[40] L. Qiu, *Research on Monitoring and Early Warning of Coal and Gas Outburst in Driving Process of Coal Roadway by EMR, AE and Gas*, China University of Mining and Technology, Xuzhou, 2018.